

# Molecular Characterization of Biodegradable Dissolved Organic Matter Using Bioreactors and [<sup>12</sup>C/<sup>13</sup>C] Tetramethylammonium Hydroxide Thermochemolysis GC–MS

SCOTT W. FRAZIER,<sup>†,§</sup>  
LOUIS A. KAPLAN,<sup>‡</sup> AND  
PATRICK G. HATCHER<sup>\*,†</sup>

*Department of Chemistry, The Ohio State University, Columbus, Ohio 43210, Stroud Water Research Center, Avondale, Pennsylvania 19311, and Institute for Terrestrial Ecology, Swiss Federal Institute of Technology Zurich, Schlieren, CH 8952, Switzerland*

Little is known about the molecular composition of the biodegradable fraction of dissolved organic matter (BDOM) in stream ecosystems. We combined plug-flow biofilm reactors, tetramethylammonium hydroxide (TMAH) thermochemolysis GC–MS, and <sup>13</sup>C-labeled TMAH thermochemolysis GC–MS to study the molecular composition of BDOM from two stream ecosystems. TMAH products derived from fatty acids, lignin, and other aromatic molecules were quantified using an internal standard approach. We applied the <sup>13</sup>C-TMAH thermochemolysis procedure to differentiate between compounds in dissolved organic matter (DOM) that had natural methoxyl groups from those that acquired methoxyl groups during the TMAH reaction. In Rio Tempisquito, a stream draining a tropical evergreen forest, and White Clay Creek, a stream draining a temperate deciduous woodlands, carbohydrates, fatty acids, and lignin contributed to the DOM and BDOM molecular composition. We observed 97 different peaks in the chromatograms of streamwater, with 57% of the peaks common to both streams. The DOM and BDOM pools from each site also contained a unique suite of compounds. Our combined use of TMAH and <sup>13</sup>C-TMAH thermochemolysis revealed that heterotrophic bacteria can selectively degrade and demethylate different types of compounds in the lignin residues of DOM. This demonstration of bacterial demethylation of lignin, an abundant and refractory plant molecule, has potential implications for global carbon cycling.

## Introduction

Dissolved organic matter (DOM) in freshwaters constitutes a complex molecular mixture that is an energy and nutrient

source for microbial heterotrophs (1) and a dynamic component of the global carbon cycle. However, the molecular composition of DOM is poorly characterized (2–4), and even less is known about the composition of biodegradable DOM (BDOM) (5, 6). This situation is largely due to a lack of analytical methods with adequate versatility to separate and identify the hydrophobic portions of DOM (7) and the sensitivity necessary in bioassays to detect biological uptake without extended incubations or an increase in substrate concentration (8–10).

The tetramethylammonium hydroxide (TMAH) thermochemolysis GC–MS procedure involves base-catalyzed hydrolysis and generates volatile products that can be related to precursor molecules (11, 12). This facilitates molecular-level investigations of DOM in general (13–17) and humic substances in particular (13, 18–24). The TMAH procedure provides a broader analytical window than CuO-oxidation used extensively for lignin analysis (25) and has fewer artifacts as compared to pyrolysis GC–MS (26). Furthermore, the inclusion of <sup>13</sup>C-labeled methylating agents in the TMAH reaction identifies the position of natural phenolic or hydroxyl functionalities from mass spectral fragmentation patterns (27) to reveal DOM structure prior to derivatization.

Combining these chemical techniques with the operation of plug-flow biofilm reactors, wherein high densities of attached streamwater microorganisms are exposed to low fluxes of organic substrates at ambient concentrations in the dark (28), provides an unprecedented characterization of streamwater DOM and BDOM molecular structure. We exploited that capability to describe DOM and BDOM composition in stream ecosystems draining a temperate deciduous forest and a tropical evergreen forest. In selecting streams from distinctly different biomes, this work provides a test of our hypothesis that differences in terrestrial vegetation at the biome-scale should result in streamwaters with distinct molecular signatures for DOM and BDOM.

## Experimental Section

**Study Sites.** Stream samples and the microorganisms used to colonize and maintain the biofilm reactors were collected from the Rio Tempisquito and White Clay Creek. Rio Tempisquito drains a virgin cloud forest and deciduous evergreen forest in the Guanacaste Province of northwestern Costa Rica, with baseflow characterized by dissolved organic carbon (DOC) concentrations that range from 0.3 to 0.7 mg C/L, 0.2 mg NO<sub>3</sub>-N/L, 0.02 mg PO<sub>4</sub>-P/L, and conductivity of 80 μS/cm (29). White Clay Creek, in the Piedmont physiographic province of southeastern Pennsylvania, drains an agricultural watershed with an intact riparian temperate, deciduous woodland, and has a baseflow characterized by DOC concentrations that range from 0.8 to 2.0 mg C/L, 3.5 mg NO<sub>3</sub>-N/L, 0.04 mg PO<sub>4</sub>-P/L, and conductivity of 200 μS/cm (30). Wet laboratories in Costa Rica and Pennsylvania are fed with a continuously flowing supply of fresh streamwater entering the buildings. These water supplies were used as the sources for colonizing the bioreactors and for samples analyzed in the work presented here.

**Plug-Flow Biofilm Reactors (Bioreactors).** The 0.6 L volume bioreactors with 2.5 h empty-bed contact times were constructed, colonized, and operated as previously described to provide the removal of DOC by an overwhelmingly

\* Corresponding author phone: (614)688-8799; fax: (614)688-5920; e-mail: hatcher.42@osu.edu.

<sup>†</sup> The Ohio State University.

<sup>‡</sup> Stroud Water Research Center.

<sup>§</sup> Swiss Federal Institute of Technology Zurich.

biological process carried out by microorganisms indigenous to the study streams (6, 28). The bioreactors were protected from light and were continuously fed filtered (75, 25, and 0.3  $\mu\text{m}$  high-temperature cured glass fiber filter cartridges in series (Balston)) streamwater and indigenous suspended microflora, pumped in a once-through, up-flow mode at 4  $\text{mL min}^{-1}$  from a reservoir. The Rio Tempisquito bioreactors were water jacketed with streamwater to maintain ambient stream temperatures (19–22 °C), while the White Clay Creek bioreactors were kept in a room that fluctuated between 12 and 22 °C throughout the year. Reservoir water was changed weekly, and the bioreactors colonized for 6 months before beginning BDOM analyses on freshly collected streamwater samples. DOC served as our analytical descriptor for the bulk DOM, and concentrations and compositions of BDOM were calculated from the differences between the bioreactor inflow and outflow samples. Bioreactor outflow samples for DOC analyses were not filtered as the sintered glass matrix and the 10  $\mu\text{m}$  bed support remove most particles. The DOM present in the outflow from the bioreactors represents the biologically refractory DOM (RDOM) that is not metabolized in the bioreactors, plus metabolic end products excreted by the organisms within the bioreactor.

**Methods.** Samples for DOC concentrations were filtered through precombusted glass fiber filters (GF/F), and the filtrates were analyzed with persulfate oxidation, assisted by UV-irradiation (Sievers 800) or Pt-catalysis and heat (OI 700 TOC). Subsamples of the GF/F filtrates from Rio Tempisquito were filtered immediately through 0.2  $\mu\text{m}$  nylon filters, acidified to pH 1 with HCl, and kept cold (5 °C) until hydrolysis and analysis of dissolved total saccharides (DTS), including neutral carbohydrates and amino sugars, by HPLC-PAD (31). The water samples for TMAH analyses (8 L) were typically collected over a 12–18-h period as the pooled outflows from three replicate bioreactors in a sterile vessel that was chilled in an ice-bath to reduce the chances for biological degradation. The 8 L was concentrated using low-temperature, low-pressure evaporation at 40 °C (Büchi rotovap) and freeze-dried to yield dried solids suitable for analysis.

TMAH thermochemolysis GC–MS analyses were performed on approximately  $100 \pm 2$  mg of the isolated total dissolved solids using the procedure described previously (14). A Hewlett-Packard 6890 GC coupled to a Pegasus II (Leco Corp., St. Joseph, MI) time-of-flight mass spectrometer operating in EI mode with a filament bias of  $-50$  V (14) was used. Selected TMAH products were quantified based upon an internal standard approach that involved the addition of eicosane to samples after the TMAH reaction but prior to product extraction by ethyl acetate, and select ions or select ion ranges to measure peak areas. Relative response factors (RRF) were generated for a collection of authentic standards. The RRF's were extended to analytes without authentic standards by assuming that structural isomers or a compound of similar structure and functional groups, eluting near the authentic standard, would have a RRF identical to that of the standard. Peak areas for TMAH products without standards were calculated using the total ion current (14).

$^{13}\text{C}$ -Labeled TMAH products were produced by the addition of 15 mg of solid  $^{13}\text{C}$ -TMAH and 100  $\mu\text{L}$  of deionized, carbon filtered, and sterile filtered water (Elgastat UHQ MK II, Elga, Bucks, England) (27, 32). We modified the equations used to determine the  $^{13}\text{C}$  enrichment of the TMAH products (27) to calculate by means of the following equations the

relative yields of the singly (SL), doubly (DL), or triply (TL) labeled products:

$$\%^{13}\text{C}_{\text{SL}} = \frac{\text{ML}}{(\text{ML} + \text{ML}_2 + \text{ML}_3)} * 100 \quad (1)$$

$$\%^{13}\text{C}_{\text{DL}} = \frac{\text{ML}_2}{(\text{ML} + \text{ML}_2 + \text{ML}_3)} * 100 \quad (2)$$

$$\%^{13}\text{C}_{\text{TL}} = \frac{\text{ML}_3}{(\text{ML} + \text{ML}_2 + \text{ML}_3)} * 100 \quad (3)$$

$$\text{ML}_2 = I_{m+2} - \frac{n_L}{n}(\text{ML} + 1)_{\text{calc}} \quad (4)$$

$$\text{ML}_3 = I_{m+3} - \frac{n_L}{n}(\text{ML}_2 + 1)_{\text{calc}} \quad (5)$$

$$(\text{ML} + 1)_{\text{calc}} = \frac{m + 1}{m} * \text{ML} \quad (6)$$

$$\text{ML}_{\text{ald}} = \frac{m}{m - H}(\text{ML}_{\text{ald}} - 1) \quad (7)$$

$\%^{13}\text{C}_{\text{SL}}$ ,  $\%^{13}\text{C}_{\text{DL}}$ , and  $\%^{13}\text{C}_{\text{TL}}$  are yields of respective labeled product as a percentage of all labeled components of that product, and ML,  $\text{ML}_2$ , and  $\text{ML}_3$  are abundances of the molecular ions for the singly, doubly, and triply labeled TMAH products, respectively. To properly account for contributions of  $^{13}\text{C}$  present at natural abundance levels, some corrections to the ML intensities were required (27).  $\text{ML}_2$  and  $\text{ML}_3$  were calculated using eqs 4 and 5, which were necessary to correct for natural  $^{13}\text{C}$  abundance of ML and  $\text{ML}_2$ .  $I_{m+2}$  is the relative abundance of the  $m/z + 2$  greater than the unlabeled TMAH product's molecular ion or fragment ion, and  $I_{m+3}$  is likewise applicable for the  $m/z + 3$  ion. Also,  $n_L$  is the number of natural carbons for the labeled compound (not including the labeled methoxy groups), whereas  $n$  is the number of carbons for the corresponding unlabeled TMAH product (including carbons from all methoxy functionalities). These terms are included to correct for the additional  $\sim 1.1\%$  per methoxy of  $^{13}\text{C}$  from the unlabeled TMAH in the corresponding labeled compound. The abundance of the  $m + 1$  ion of the labeled compound,  $(\text{ML} + 1)_{\text{calc}}$ , is calculated by determining the ratio of natural  $^{13}\text{C}$  abundance ( $m + 1$ ) relative to the molecular ion  $m$  from the unlabeled TMAH product and then by multiplying this ratio by ML (eq 6).  $(\text{ML}_2 + 1)_{\text{calc}}$  is calculated in the same manner by substituting  $\text{ML}_2$  for ML in eq 6.

For 3,4-dimethoxy benzaldehyde (G4), eq 7 was used to calculate ML (here  $\text{ML}_{\text{ald}}$ ) as a result of the substantial  $m - H$  peak of  $\text{ML}_2$  that interferes with the  $\text{ML}_{\text{ald}}$  abundance determination. The ratio  $m/(m - H)$  was determined from the unlabeled TMAH product.  $(\text{ML}_{\text{ald}} - 1)$  is the  $m - H$  abundance of the singly labeled TMAH product. For all other compounds, the  $m - H$  peak was found to be insignificant, and no correction was required. Only  $^{13}\text{C}$ -TMAH results from the White Clay Creek DOM and RDOM are presented as lack of sufficient sample precluded a similar analysis of the Rio Tempisquito samples.

## Results and Discussion

**Bulk Characteristics of DOM and BDOM.** The DOC concentrations in the bioreactor feedwater from the Rio Tempisquito ( $0.65 \pm 0.02$  mg C/L ( $n, 3$ ) [mean  $\pm$  SD ( $n$  sample replicates)]) are consistent with concentrations observed for that stream at baseflow (29). Outflow DOC concentrations from the three replicate Rio Tempisquito bioreactors had a coefficient of variation (cv) of 2.6% and averaged  $0.60 \pm 0.02$

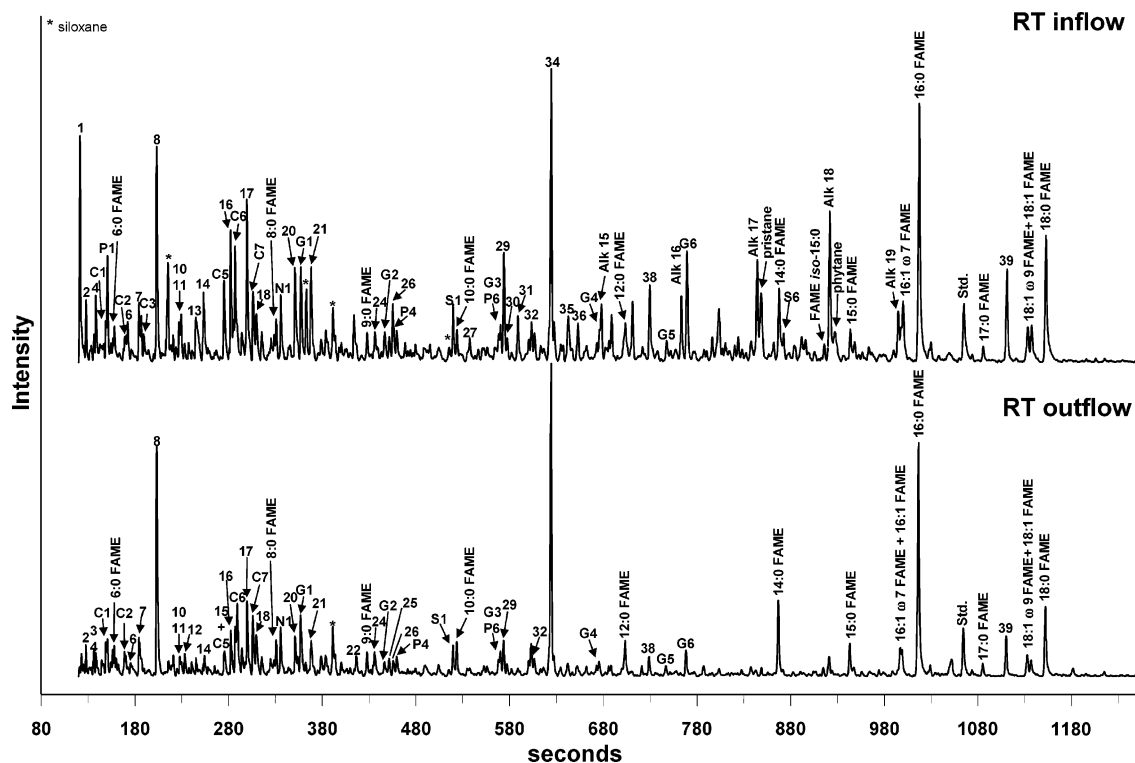


**FIGURE 1.** TMAH thermochemolysis GC-MS chromatograms (TIC) for Rio Tempisquito (RT) bioreactors inflow and outflow DOM. Peak identifications are given in Table 1. "\*" corresponds to a series of methyl siloxanes seen in the inflow DOM. FAME = fatty acid methyl esters, Alk = alkanes, std = internal standard eicosane.

mg C/L (*n*,2), resulting in a biodegradable DOC (BDOC) concentration of 0.05 mgC/L, or 7.7% of the streamwater DOC. DOC concentrations in the bioreactor feed from the White Clay Creek ( $5.75 \pm 0.07$  mg C/L (*n*,4)) are consistent with that stream under stormflow conditions (33). Outflow from a single White Clay Creek bioreactor was collected for analysis and averaged  $2.44 \pm 0.01$  mg C/L (*n*,3), resulting in a BDOC concentration of 3.00 mg C/L, or 52.2% of the streamwater DOC. Previous analyses of BDOC with White Clay Creek bioreactors showed that outflow measurements from four replicate bioreactors on six different dates over a 4-month period had an average cv of 5.5% (6).

Dissolved total saccharide concentrations of  $395 \pm 26$  nM (*n*,3) in Rio Tempisquito streamwater, including fucose, rhamnose, arabinose, glucosamine, galactose, glucose, mannose, and xylose, declined by 62% in passage through the bioreactors (outflow concentrations equaled  $159 \pm 6$  nM (*n*,3)). Uptake of individual carbohydrate molecules within the DTS pool ranged from 82% of the glucosamine to 30% of the glucose.

#### Molecular Composition of DOM, RDOM, and BDOM.

We observed 97 different peaks in the chromatograms of streamwater, including 82 from Rio Tempisquito, 69 from White Clay Creek, and 55 that were common to both streams. We have organized the TMAH products into sections based on their potential biomolecular precursors (Figures 1–3, Table 1). Potential precursors include carbohydrates, lignin, fatty acids, alkanes, and N-containing compounds, although we recognize that precursors for a given TMAH product may not be unique, resulting in some overlap, and there are numerous peaks with unknown precursors. Some products of uncertain origins are probably general products from more than one precursor. These include methoxy butanes and pentanes, butanoic and pentanoic acid, diacid methyl esters, often with methoxy constituents, trimethoxy benzenes and trimethoxy toluenes, methoxy benzene, 1,2- and 1,4-dimethoxy benzenes, and benzyl methyl ether.

White Clay Creek DOM had several dominant peaks: 3-methoxy pentane (peak 2); benzyl methyl ether (peak 8); 1,4-dimethoxy benzene (peak 21); 1,3,5-trimethoxy benzene (peak 32); and the 16:1  $\omega$ 7 and 16:0 FAMES. Most prominent among the Rio Tempisquito streamwater TMAH products were *p*-xylene (peak 1), benzyl methyl ether (peak 8), and 16:0 FAME. Peak 34, 2,6-di-*tert*-butyl-4-methyl phenol (BHT), is a contaminant artifact from the extraction solvent. Among the dominant peaks, only the FAMES can be attributed to definite precursors.

There was a reduction in area for nearly all peaks in the Rio Tempisquito and White Clay Creek outflow samples, as compared to inflow, including peaks in the early and mid-retention times corresponding to carbohydrate- and lignin-derived products as well as other nonspecific TMAH products. Only 2-methoxy-3-methyl butyric acid methyl ester (peak 5) and 1,1'-(1-methylidene) bis-4-methoxy benzene (peak 39) were clearly enhanced in the bioreactor outflow as compared to the streamwater. Even though the FAME distribution in the stream samples suggested a bacterial origin for these molecules, there was a notable difference in the FAME distributions between the inflow and outflow samples, resulting from a greater reduction of the mono-unsaturated FAMES within the bioreactors.

Carbohydrate-derived TMAH products were observed both early in the chromatograms, including methyl and methoxy cyclopenten-1-ones, furanones, and pyranones, and later in the chromatograms, indicating higher molecular weight carbohydrate derivatives. The latter were difficult to precisely identify by comparison with library spectra, but likely retain more information regarding precursor structures than the former carbohydrate-derived products (34). Also present throughout the early to mid retention times of the chromatograms were many compounds believed to be lignin-derived, such as methoxy-substituted aromatic products. However, many of these products can result from other biomolecules such as carbohydrates, tannins, and proteins

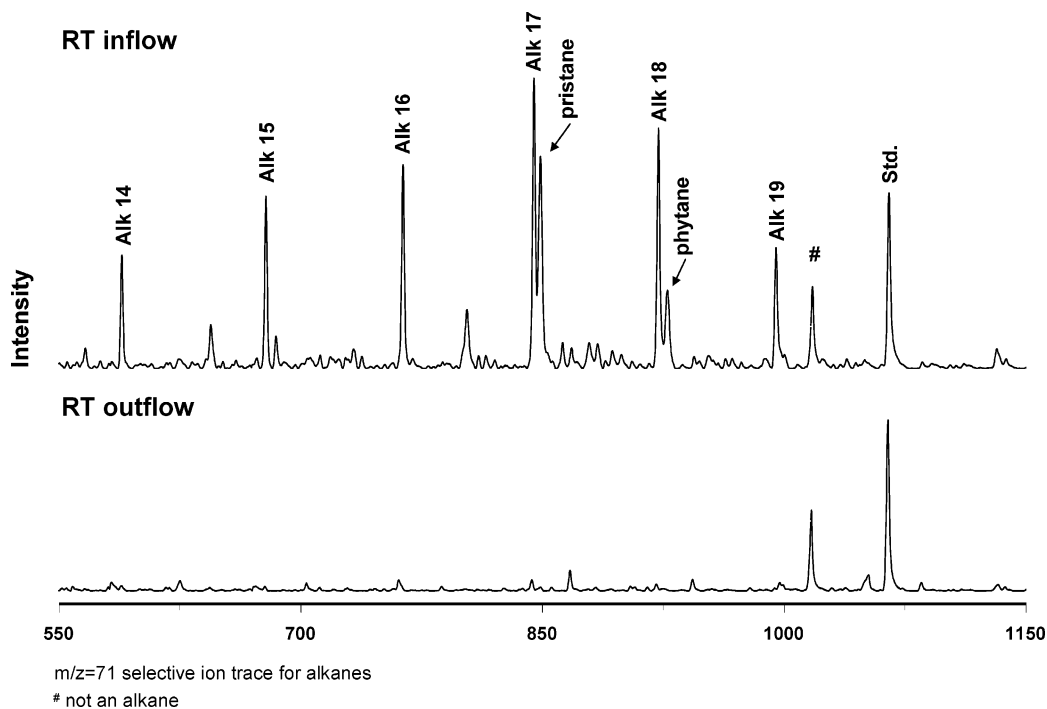


**FIGURE 2. TMAH thermochemolysis GC-MS select ion traces (SIC,  $m/z = 71$ ) for alkanes for the RT bioreactors inflow and outflow DOM. “#” denotes peaks that do not correspond to alkanes.**

(15, 34). Although not strongly represented in either stream, heterocyclic N-containing compounds were present in the mid retention times of the chromatograms. Some of these compounds may have been derived from lignin, as we have demonstrated that lignin standards added to DOM samples prior to the TMAH reaction generated heterocyclic N-containing TMAH products (14). A series of *n*-FAMES with an even over odd predominance, accompanied by several branch-chain isomers and unsaturated FAMES, was present consistently throughout the TMAH chromatograms of DOM. This series ranged from hexanoic acid through tetratricoic acid, methyl esters. In general, the distribution of FAMES was similar between the DOM and RDOM samples and is indicative of bacteria because the distribution was dominated by saturated FAMES with some monoenoic FAMES (predominantly 16:1  $\omega$ 7 and 18:1  $\omega$ 9). Substantial amounts of iso and anteiso 15:0 FAMES were also present, which suggests that there were contributions from gram-positive bacteria (35). There was little contribution from eukaryotes as indicated by the lack of polyunsaturated fatty acids, although their absence could be expected because these fatty acids are quickly metabolized (36). Contributions of fatty acids from higher plants were minimal as noted by the lack of higher molecular weight fatty acids ( $>C_{24}$  units).

The FAME results indicate that products of microbial lysis (primarily bacterial) may significantly contribute to the DOM pool. This has been observed for dissolved organic nitrogen in marine waters (4), but a similar process has not been reported for freshwaters. GF/F filtration allows most of the bacteria suspended in streamwater to pass into the filtrate, so we were unable to distinguish TMAH products from intact cells from products that result from the lysis or excretion of bacterial cells. However, this series of FAMES was present in duplicate samples from Rio Tempisquito that were sterile filtered to remove all bacteria, so our results suggest that the FAMES were in the dissolved phase and the result of bacterial death or lysis.

Another notable series of compounds for the DOM sample from Rio Tempisquito was the alkanes ranging from tetradecane to nonadecane (Figure 2). The series showed an

odd over even predominance in the select ion trace ( $m/z = 71$ ) and complete removal within the bioreactor. This contradicts the notion that alkanes, including highly branched alkanes, are highly resistant to microbial degradation (37) and contrasts with the slow degradation of lower molecular weight alkanes within the water column of lakes during sedimentation as well as within sediments upon deposition and burial (38–40). The relatively low molecular weight distribution of this series, centered around the  $C_{17}$  alkane, suggests algal/microbial sources as opposed to higher plant sources such as cuticle waxes (38, 40), which while present in the tropical plants have low solubility. Pristane and phytane have been observed in lakes, are characteristic of algal origins, and are thought to result from transformations of phytol, the isoprenoid side-chain of chlorophyll a (38, 40).

Some compounds in the chromatograms were not derived from the streamwater DOM, but are artifacts of the TMAH reaction. The artifacts that we know of include 4,6-dimethyl-3,5-dioxo-2,3,4,5-tetrahydro triazine, 1,3,5-trimethyl-1,3,5-triazine-2,4,6-trione, pyrimidinediones, pyrrolidinediones, and caffeine. These compounds were not included in our figures or table. Two artifacts that do appear in Figures 1 and 3, peak 34, derived from BHT in the extraction solvent, and peak 39, a benzene dimer (1,1'-(1-methylidene) bis-4-methoxy benzene, were prominent peaks in the chromatograms from both sites. The latter product derives from bisphenol A (4,4'-(1-methylethylidene)bis-phenol (CAS 80-05-7)), which is used in the manufacturing of polycarbonate and was likely introduced from the polycarbonate containers used for storage and shipping of the streamwater samples.

**Quantitative Comparison of TMAH Products from DOM and RDOM.** The yields (concentrations) of 37 TMAH products quantified in the inflow and outflow to the bioreactors were used to calculate the contributions of these products to the concentrations of BDOM in the Rio Tempisquito (Figure 4) and White Clay Creek (Figure 5). The percent of each compound biodegraded is also listed in the figures. Concentrations of individual compounds from Rio Tempisquito declined on passage through the bioreactors by 35–82%, and those from White Clay Creek declined by 12% to ~100%.

**TABLE 1. Peak Identifications for Rio Tempisquito and White Clay Creek DOM and BDOM Samples**

Peak	Compound	Peak	Compound
	<b>TMAH products of uncertain origin</b>		<b>Potential lignin derived TMAH products</b>
1	p-xylene	P1	methoxy benzene
2	3-methoxy pentane	P3	1-ethenyl-4-methoxy benzene
3	4-methyl pentanoic acid, methyl ester	G1	1,2-dimethoxy benzene
4	2-hydroxy-3-methyl butyric acid, methyl ester	G2	3,4-dimethoxy toluene
5	2-methoxy-3-methyl butyric acid, methyl ester	P4	4-methoxy benzaldehyde
6	4-methoxy butanoic acid, methyl ester	S1	1,2,3-trimethoxy benzene
7	benzaldehyde	G3	4-ethenyl-3,4-dimethoxy benzaldehyde
8	benzyl methyl ether	P6	4-methoxy benzoic acid, methyl ester
9	1-methoxy-2-methyl benzene	S2	1,2,3-trimethoxy-5-methyl benzene
10	decahydro naphthalene	G4	3,4-dimethoxy benzaldehyde
11	1-methoxy-3-methyl benzene	G5	1-(3,4-dimethoxy phenyl) ethanone
12	methoxy butanoic acid, methyl ester	G6	3,4-dimethoxy benzoic acid, methyl ester
13	2-ethyl hexanoic acid, methyl ester	S6	3,4,5-trimethoxy benzoic acid, methyl ester
14	butanedioic acid, dimethyl ester		<b>Fatty acid, methyl esters (FAME)</b>
15	acetophenone	6:0	hexanoic acid, methyl ester
16	methyl butanedioic acid, dimethyl ester	8:0	octanoic acid, methyl ester
17	benzoic acid, methyl ester	9:0	nonanoic acid, methyl ester
18	methyl decahydro naphthalene	10:0	decanoic acid, methyl ester
19	unknown compound (m/z 42, 127, 58)	12:0	dodecanoic acid, methyl ester
20	pentanedioic acid, dimethyl ester	13:0 br	methyl tridecanoic acid, methyl ester
21	1,4-dimethoxy benzene	14:0	tetradecanoic acid, methyl ester
22	methyl benzeneacetic acid, methyl ester	iso 15:0	12-methyl tetradecanoic acid, methyl ester
23	methyl decahydro naphthalene	anteiso	
24	unknown compound (m/z 42, 127, 58, 142)	15:0	11-methyl tetradecanoic acid, methyl ester
25	1,4-dimethoxy-2-methyl benzene	15:0	pentadecanoic acid, methyl ester
26	hexanedioic acid, dimethyl ester	16:1 ω7	9-hexadecenoic acid, methyl ester
27	3-methoxy benzoic acid, methyl ester	16:0	hexadecanoic acid, methyl ester
28	4-ethyl-1,2-dimethyl benzene	17:1	heptadecenoic acid, methyl ester
29	1,2,4-trimethoxy benzene	17:0	heptadecanoic acid, methyl ester
30	3-phenyl-2-propenoic acid, methyl ester	18:1	octadecenoic acid, methyl ester
31	methoxy benzeneacetic acid, methyl ester	18:1 ω9	9-octadecenoic acid, methyl ester
32	1,3,5-trimethoxy benzene	18:0	octadecanoic acid, methyl ester
33	3-methoxy-4-methyl benzoic acid, methyl ester		<b>Alkanes</b>
34	2,6-di-tert-butyl-4-methyl phenol (BHT)	Alk 15	C <sub>15</sub> alkane
35	octanedioic acid, dimethyl ester	Alk 16	C <sub>16</sub> alkane
36	1,2,3-trimethoxy-5-(2-propenyl) benzene	Alk 17	C <sub>17</sub> alkane
37	2-methoxy benzenepropanoic acid, methyl ester	pristane	C <sub>19</sub> branched alkane (pristane)
38	nonanedioic acid, dimethyl ester	Alk 18	C <sub>18</sub> alkane
39	1,1'-(1-methylidene) bis-4-methoxy benzene	phytane	C <sub>20</sub> branched alkane (phytane)
	<b>Carbohydrate derived TMAH products</b>	Alk 19	C <sub>19</sub> alkane
C1	2-methyl-2-cyclopenten-1-one		<b>N containing compounds</b>
C2	3,4-dimethyl-2-cyclopenten-1-one	N1	unknown heterocyclic N compound (56,141,156)
C3	dihydro 4-methyl-2(3H) furanone	N2	3-ethyl-1,3-dimethyl-2,5-pyrrolidinedione
C4	tetrahydro 2H-pyran-2-one	N3	1,3,5-trimethyl-2,4(1H,3H) pyrimidinedione
C5	2,3,4-trimethyl-2-cyclopenten-1-one		
C6	1-cyclohexyl ethanone		
C7	2-ethyl-3-methoxy-2-cyclopenten-1-one		
C8	1,5-anhydro-2,3,4,6-tetra-o-methyl-d-mannitol		

The most abundant TMAH compounds were the most effectively degraded during passage through the bioreactors, suggesting acclimation of the indigenous bacterial communities to exploit the most abundant carbon and energy sources. For the Rio Tempisquito, the sum of quantified aromatic products contributes 6.1 μg/L to the inflow, 2.1 μg/L to the outflow, and, by difference, 4.0 μg/L to the BDOM pool metabolized within the bioreactors. Subtracting the nonlignin products from these total aromatic products provides an estimate of the lignin contributions to the inflow (3.5 μg/L), outflow (1.3 μg/L), and BDOM (2.2 μg/L) for the Rio Tempisquito. Similar treatment of the FAME products shows 5.0 μg/L in the inflow, 2.2 μg/L in the outflow, and 2.8 μg/L of BDOM.

Each class of compounds had higher concentrations in White Clay Creek compared to Rio Tempisquito, and aromatic products contributed 8.9 μg/L in the inflow, 3.7 μg/L in the outflow, and 5.2 μg/L of BDOM. A slightly lower percentage of the aromatic products from White Clay Creek was derived from lignin as compared to Rio Tempisquito, with inflow contributing 4.6 μg/L, outflow contributing 1.8 μg/L, and 2.8 μg/L of BDOM. FAMES contributed 7.3 μg/L to the inflow, 2.2 μg/L to the outflow, and 5.0 μg/L of BDOM.

The carbohydrate precursors for 1,4-dimethoxy benzene and 1,2,4-trimethoxy benzene were the most effectively degraded in the White Clay Creek bioreactors, while the lignin precursor for 3,4-dimethoxybenzoic acid methyl ester was most effectively degraded in the Rio Tempisquito bioreactors. Other possible carbohydrate-derived products such as the dimethoxy toluenes were not effectively degraded, confirming our prior observations of a selectivity in carbohydrate degradation (6, 33). The products of undetermined sources were not as effectively degraded.

Several fatty acids contributed to the BDOM in these stream ecosystems. The 16:1ω7, 16:0, and 18:1ω9 FAMES were the most predominant FAMES in the DOM and were the most efficiently degraded by the heterotrophic bacteria, whereas the other low-molecular weight fatty acids were degraded to a lesser degree. These results are consistent with prior studies that found unsaturated fatty acids more biodegradable than the *n*-fatty acids, that is, saturated fatty acids (35, 37–39). Both iso and anteiso 15:0 fatty acids were degraded more effectively within the bioreactors than the *n*-fatty acids, with a corresponding decrease in the ((iso 15:0 + anteiso 15:0)/16:0) ratio in passage through the bioreactors, indicating selective removal of terminally branched fatty

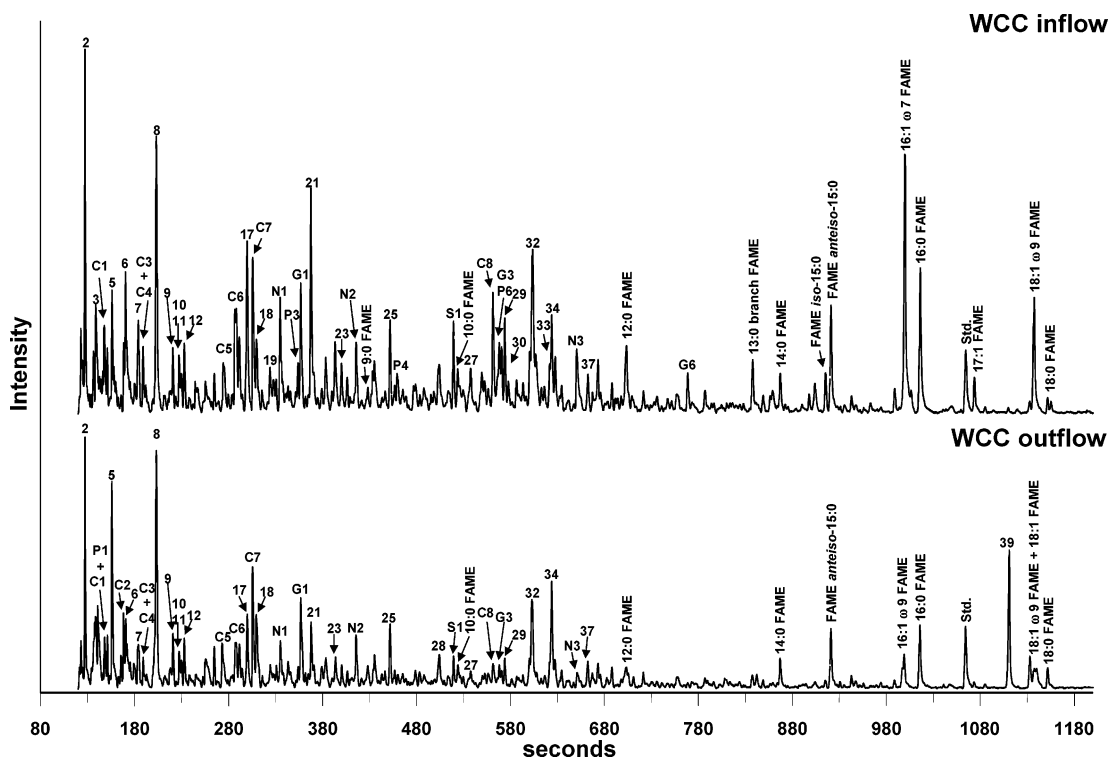


**FIGURE 3.** TMAH thermochemolysis GC–MS chromatograms (TIC) for White Clay Creek (WCC) bioreactors inflow and outflow DOM. Peak identifications are given in Table 1, and abbreviations are the same as those noted in Figure 1.

acids. These results demonstrate that the fatty acid composition of DOM can be altered upon bacterial degradation, although the distribution from fatty acids is, in general, qualitatively similar between the DOM and RDOM samples (Figures 4 and 5). Bacteria within the bioreactors likely affect the fatty acid composition of DOM by both selectively degrading certain components of DOM while contributing others through excretion and lysis.

We have not extrapolated the above quantitative data on TMAH products to estimate the percentages of DOC in both streams accounted for with the TMAH method. Additionally, while it is clear that carbohydrates, lignin, and fatty acids contributed to BDOC in both streams, we have not used these data to characterize the overall molecular composition of the BDOC pool. These calculations would be logical extensions of this study; however, developing authentic standards to generate RRFs is difficult, recovery of authentic lignin is low, and recovery estimates for other classes of compounds have not been performed. At present, we only have quantitative RRF estimates for 53–67% of the TMAH products. While the RRFs for closely related compounds are very similar, over the range of compounds tested, there was a 22-fold difference (14), limiting our ability to extrapolate beyond the current list of TMAH products with confidence. Recovery of a single lignin standard subjected to the TMAH procedure was estimated as  $3.3\% \pm 0.2$  (mean%, SD), a value that is consistent with other degradative techniques (14). Efficiency estimates for carbohydrates, proteins, tannins, and fatty acids have not been performed, and potentially significant differences in compound-specific efficiencies are expected.

The TMAH technique is especially powerful when used in direct comparisons of particular TMAH products, such as the differences between lignin-derived molecules detected in the inflow and outflow samples from bioreactors. Molecular-level analyses that identify the contributions of lignin-derived degradation products as originating from syringyl (S), guaiacyl (G), or *p*-hydroxyphenyl (P) parent material have been used to identify the nature of the plant sources of lignin

in DOM. The S/G and P/G ratios for Rio Tempisquito (0.41; 0.46, respectively) and White Clay Creek (0.46; 0.75, respectively) are indicative of lignin that originates predominantly from nonwoody gymnosperms, but the surrounding vegetation is predominantly woody and nonwoody angiosperms. It is possible that, in stream ecosystems, the S/G and P/G ratios are modified through selective metabolism in riparian soils or within the stream itself, and thus bacterial degradation could obscure information regarding terrestrial sources of lignin. To the extent that protein degradation yields *p*-hydroxyphenyl, the assumption that *p*-hydroxyphenyl products are only lignin-derived would be violated and that too would influence the P/G ratio.

The acid-to-aldehyde ratio of guaiacyl-derived compounds from lignin (Ad/Al)<sub>G</sub> has been used to assess the degree of degradation for lignin as microbes oxidize the  $\alpha$ -carbons of aldehydes to produce acids (41). Thus, as degradation proceeds, the (Ad/Al)<sub>G</sub> is expected to increase, and this has been demonstrated with CuO-oxidation (40, 41) and TMAH thermochemolysis (20) of terrestrially degraded lignin. These relationships were derived from terrestrial sources of organic matter that had undergone fungal decomposition. In these bioreactors, where bacteria are the primary decomposers, (Ad/Al)<sub>G</sub> decreased from 2.00 in the Rio Tempisquito inflow to 1.09 in the outflow, and from 0.74 in the White Clay Creek inflow to 0.35 in the outflow. These results suggest that the bacteria in the bioreactors preferentially metabolize oxidized methoxy aromatic structures over the more reduced material and presumably less degraded lignin. Alternatively, these ratios were developed using CuO oxidation and may not directly apply to TMAH thermochemolysis. Hatcher et al. (20) did find that the acid:aldehyde ratios from TMAH correlate well with those from CuO, and TMAH yielded higher values, but the applicability of TMAH-derived ratios to diagenetic history has not been investigated.

In fact, organisms within both the Rio Tempisquito and the White Clay Creek bioreactors did utilize the more oxidized precursors for 3,4-dimethoxybenzoic acid methyl ester (peak

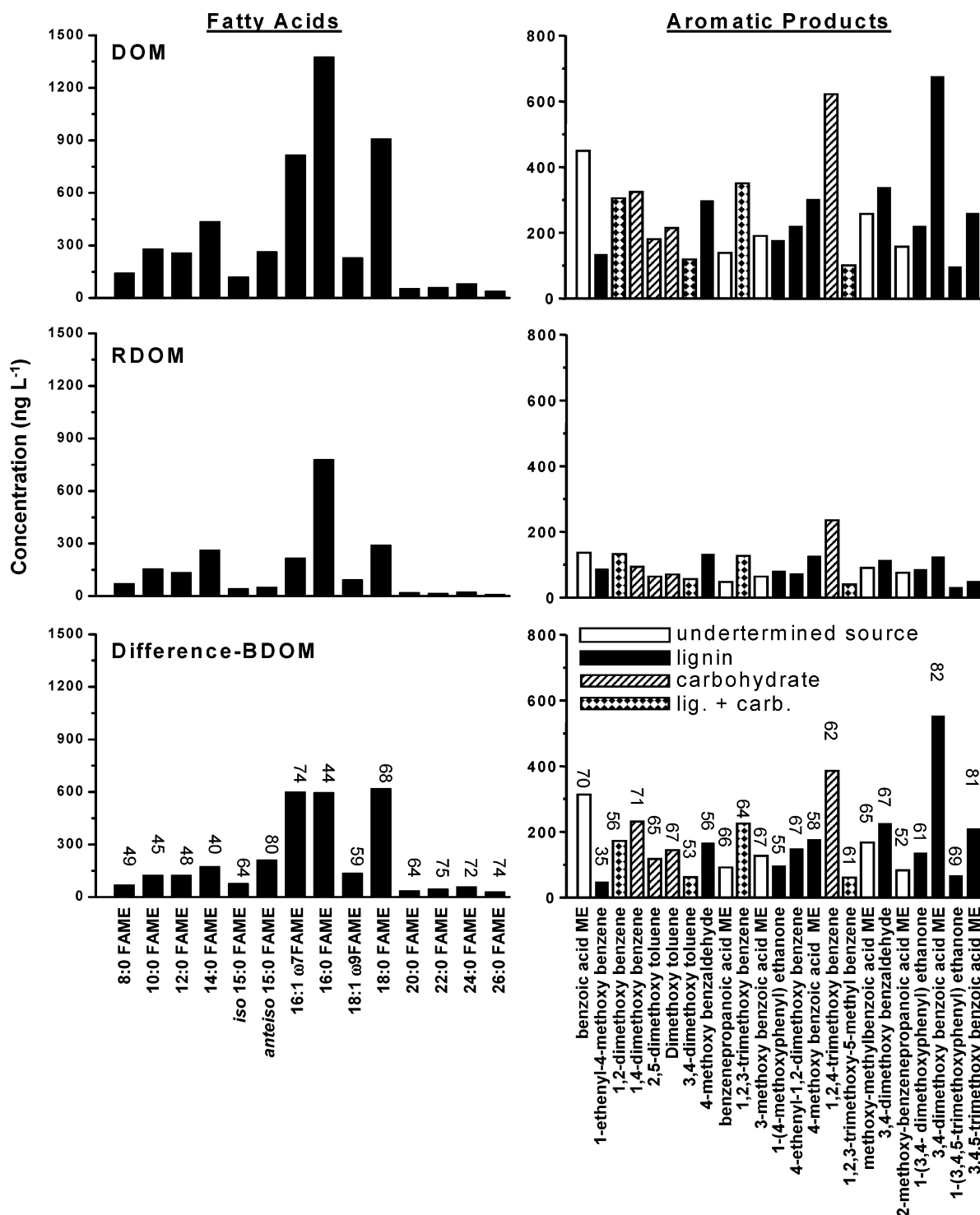


**FIGURE 4.** Yields of fatty acids and aromatic TMAH thermochemolysis products for the Rio Tempisquito (RT) bioreactors DOM (inflow) and RDOM (outflow) and the difference (BDOM). Yields are calculated as ng L<sup>-1</sup>. ME = methyl ester, lig. + carb. = derived from either lignin or carbohydrates. Numbers above bars indicate percent of biodegradation for the respective compounds.

G6) and 3,4,5-trimethoxybenzoic acid methyl ester (peak S6) more effectively than the more reduced lignin precursors that produce aldehyde and ketone TMAH products (Figures 4 and 5). Also, the degradation of 3,4,5-trimethoxybenzoic acid by *Pseudomonas spp.* has been found only to occur in the presence of 3,4-dimethoxybenzoic acid, and they were degraded at nearly equivalent rates (43), which is confirmed by our observations. The degradation of lignin residues requires an initial formation of epoxides to cleave aromatic ring structures (43). Bacterial cleavage of aromatic rings is facilitated when a carboxyl group or an easily oxidized

functionality to a carboxyl group is accompanied by a hydroxyl group in the *para* position (44). The degradation of such lignin subunits, which likely produce 3,4-dimethoxybenzoic acid methyl ester upon treatment with TMAH, may occur preferentially as compared to the lignin residues in DOM that have more reduced side-chains and that produce 3,4-dimethoxy benzaldehyde upon treatment with TMAH. Therefore, if side-chain oxidation of the more reduced lignin residues is slower than ring cleavage of the more oxidized lignin residues, the (Ad/Al)<sub>G</sub> would decrease upon degradation by heterotrophic bacteria.

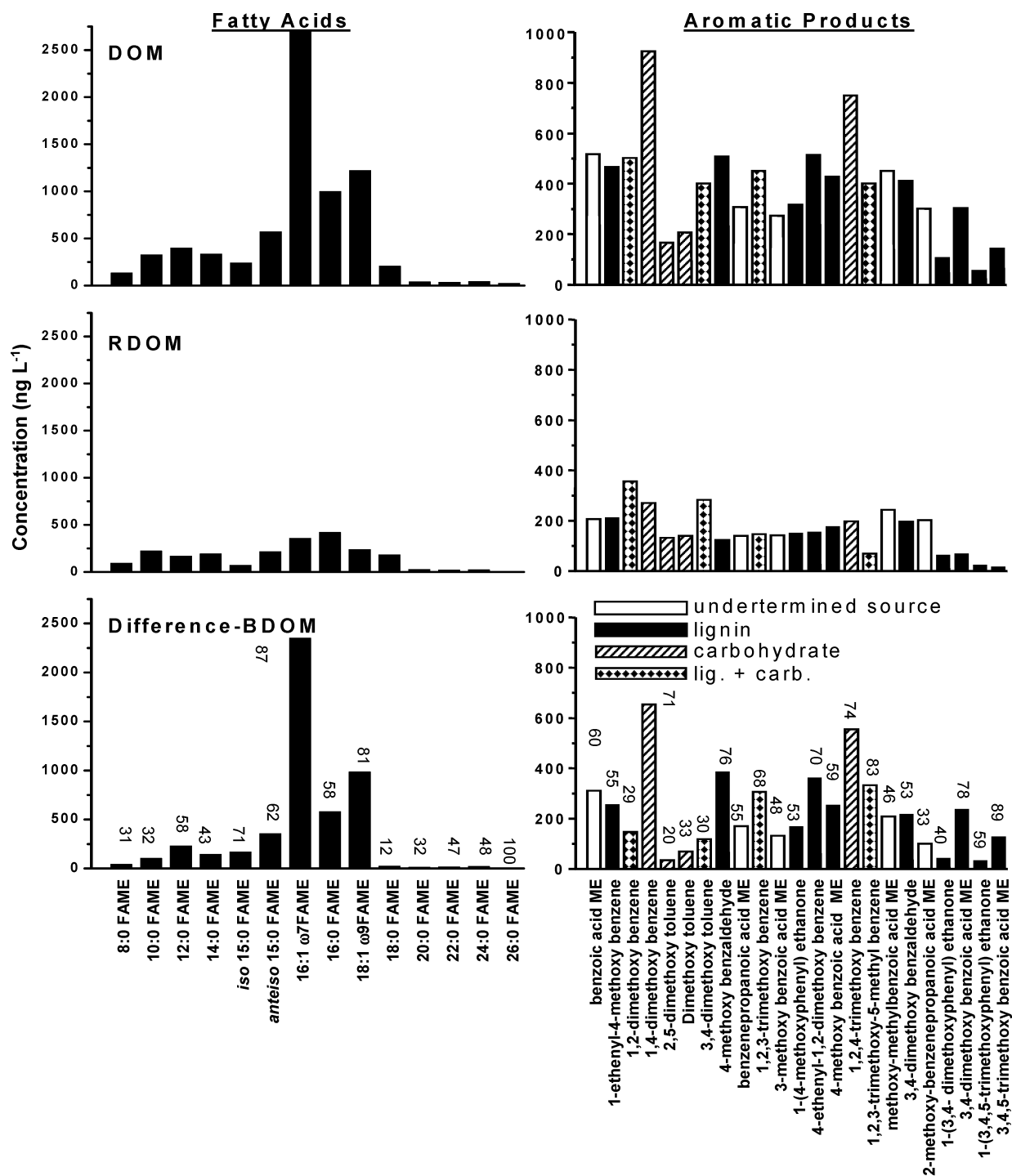


**FIGURE 5.** Yields of fatty acids and aromatic TMAH thermochemolysis products for the White Clay Creek (WCC) bioreactors DOM (inflow) and RDOM (outflow) and the difference (BDOM). Yields are calculated as ng L<sup>-1</sup>, and abbreviations are the same as those noted in Figure 4. Numbers above bars indicate percent of biodegradation for the respective compounds.

So, summarizing the results of our TMAH study of bioreactor-treated DOM, we found that lignin contributes substantially to the BDOM fraction (along with carbohydrates, fatty acids, and proteins). This is intriguing because lignin is considered a relatively refractory biomolecule. Saturated fatty acids are degraded similarly or less effectively than other compounds observed in these DOM samples. This is surprising because fatty acids are considered relatively metabolically labile as compared to many forms of organic matter. It may be that these fatty acids are associated with the refractory portions of the DOM and are protected. On a molecular level, the catabolic activities of indigenous bacterial

communities appear to be unique in the types of organic matter they utilize. For example, differences in DOM degradation are observed for the precursors of nonlignin compounds (carbohydrates, tannins, and other sources), and unique changes are observed in the biodegradation of the precursors producing *p*-hydroxy phenyl, guaiacyl, and syringyl TMAH products, suggesting selective degradation between different forms of lignin. The (Ad/Al)<sub>G</sub>, which indicates the degree of terrestrial degradation and is supposed to increase with increasing degree of degradation, decreases upon bacterial degradation associated with the bioreactors.

This indicates that bacteria display a preference for the more oxidized lignin molecules in DOM as compared to the more reduced forms leading to a depletion of these oxidized forms in RDOM products. However, both sites share some commonalities in that the most abundant compounds in the TMAH products of DOM also contributed the most to the TMAH products of BDOM. This suggests that the indigenous microbial communities represented in the bioreactors may be adapted or selected to use the most abundant source of energy.

**<sup>13</sup>C-TMAH Thermochemolysis GC-MS.** The <sup>13</sup>C-TMAH thermochemolysis GC-MS procedure extends our investigation of the effects of bacterial degradation on White Clay Creek DOM molecular composition and can distinguish between compounds having methoxy functionalities prior to TMAH thermochemolysis from those that acquire methoxyl groups during the TMAH procedure. Noting the presence of 100% <sup>13</sup>C methylation in a compound by mass spectrometry is a clear determination that the precursor was not methylated prior to <sup>13</sup>C-TMAH thermochemolysis. Hence, by analysis of the <sup>13</sup>C-TMAH products, we are able to observe molecules in White Clay Creek DOM that possess natural methoxy groups (these would not be labeled because we assume no exchange) and also how bacterial degradation affects these molecules, presumably by demethylation of methoxyl groups or by transformation to carboxylated products in which cases the TMAH would add a labeled methyl group. In the following discussion, we use the term precursor to refer to the compound from which the <sup>13</sup>C-labeled TMAH product derives.

The molecular weight of the numerous isomers of dimethoxy benzene is 138 when both methoxyl groups are unlabeled and 140 when both methoxyl groups are labeled (Figure 6A). If the precursors in DOM or RDOM for the dimethoxy benzene products have two preexisting methoxyl groups prior to <sup>13</sup>C-TMAH, then they will not be labeled and the molecular weight will remain 138. However, if the precursors for the dimethoxy benzene exist in DOM or RDOM as demethylated analogues prior to TMAH thermochemolysis, then they will acquire one and possibly two <sup>13</sup>C methyl groups during <sup>13</sup>C-TMAH thermochemolysis, and their molecular ions in the mass spectra will be at *m/z* 139 and 140, respectively. By using eqs 2-7 and measurements of relative molecular ion intensities, the relative contributions from each of the precursors can be determined. These estimates are listed for each of the TMAH products in Figure 6A-C.

For the compounds in the following discussion, listed in Table 1, there were no preexisting methoxy groups at sites of methylation in precursors, and they were, therefore, all initially phenolic, acidic, or ester linked. The <sup>13</sup>C-labeled methyl ester group for all FAMES and diacid methyl esters were either free acids or ester linked to molecules larger than a methyl group. It is possible that a preexisting methyl ester would be transesterified and the methyl replaced by a labeled methyl group; however, to our knowledge, methyl esters of fatty acids are not known to exist as such in DOM. The mass spectra for the furanose carbohydrate products are identical to spectra from use of unlabeled TMAH except for 2-ethyl-3-methoxy-2-cyclopenten-1-one (peak C7) where 100% of the product was enriched with one <sup>13</sup>C-label. The general absence of labeled products is expected for carbohydrates. The dimethoxy-methyl benzene isomers (peaks 25, G2) and 3,4,5-trimethoxy toluene (peak S2) are fully labeled and thus exhibit no original methoxy groups prior to the reaction with labeled TMAH. These compounds likely derive from precursors such as carbohydrates and tannins, so the lack of preexisting methoxy groups is consistent with these sources. Some of the products of uncertain or less specific origin, such as benzyl methyl ether (peak 8), methoxy-methyl benzenes (peaks 9,10), methoxy benzene acetic acid, methyl

esters (peak 31, peak not shown), and benzoic acid, methyl ester (peak 17) are also fully <sup>13</sup>C methylated. Benzene propanoic, propenoic, and their methoxy-substituted methyl esters (peaks 30 and 37) have been found to derive from proteins (15), so the lack of any preexisting methoxy groups is consistent with these origins. Methoxy benzene (peak P1), 1-ethenyl-4-methoxy benzene (peak P3), 4-methoxy benzaldehyde (peak P4), and 4-methoxybenzoic acid, methyl ester (peak P6) can derive from proteins and lignin, and their presence as the fully labeled methoxy-substituted products is consistent with these sources. Compounds such as 3-methoxybenzoic acid, methyl ester (peak 27), and 3-methoxy-4-methyl benzoic acid, methyl ester (peak 33) result from undetermined sources and are not methylated prior to treatment with <sup>13</sup>C-TMAH. Compound 1,1'-(1-methylidene) bis-4-methoxy benzene (peak 39 with both methoxy groups labeled) derives from bisphenol A, a well-known contaminant derived from polycarbonate plastics.

The mass spectra for 1,2-, 1,4-, and 1,3-dimethoxy benzenes are presented in Figure 6A-C for DOM treated by labeled TMAH. Treatment of intact lignin with <sup>13</sup>C-TMAH is normally expected to produce subunits that have at least one <sup>13</sup>C-labeled methoxy group as the reaction cleaves the  $\beta$ -aryl ether unit and methylates the ether-linked oxygen on the aromatic ring. If the lignin is partially degraded, having been singly demethylated to a hydroxy aromatic ether, the <sup>13</sup>C-TMAH will introduce two <sup>13</sup>C-labeled methoxy groups for the product. Thus, we can determine the extent to which this has occurred by measuring the proportion of label incorporation, assuming that other substances such as tannin do not interfere with this concept. Tannin can yield similar products. Likewise, the dimethoxy phenolic ether units of lignin containing syringyl subunits can become fully or partially demethylated during microbial degradation, and they can receive up to three labeled methoxy groups during <sup>13</sup>C-TMAH thermochemolysis. As above, the presence of hydrolyzable tannins containing gallic acid subunits can interfere with this as they can yield aromatic units with three labeled methoxyl groups. Here, we have assumed that tannins are minor contributors but realize that their presence in significant abundance can compromise the conclusions we reach. We have no independent way of ascertaining their contribution.

From the mass spectra and with the above caveat, we determine that the 1,2-dimethoxy benzene product (peak G1) from DOM derives from lignin that is comprised of 32.2% 2-methoxy phenolic ether subunits (normal lignin containing one methoxy group that is not replaced by a labeled methoxy group) and 67.8% hydroxy phenolic ethers, or lignin whose subunits have undergone mostly demethylation, and the <sup>13</sup>C-TMAH has now introduced two labeled methoxy groups (Figure 6A). There is a slight shift toward more of the doubly labeled subunits in the RDOM relative to the DOM; however, the difference is not significant statistically when one considers peak intensity reproducibility in mass spectrometry to be on the order of 5%. The product 1,2-dimethoxy benzene, existing as catechol or hydroxy phenolic ether subunits prior to methylation, has been found to be a TMAH product from degraded lignin (13) but can also derive from carbohydrates (34). We also find, in preliminary experiments, that 1,2- and 1,4-dimethoxy benzene are produced in equivalent amounts from treatment of carbohydrates (cellulose) with TMAH (unpublished data). In addition, the doubly labeled 1,2-dimethoxy benzene could also derive from tannins, as mentioned above.

Nearly all of the 1,4-dimethoxy benzene product from both the DOM and the RDOM samples derives from a 1,4-dihydroxy benzene, or its hydroxy phenolic ether analogue, precursor subunit (Figure 6B). Because 1,4-dimethoxy benzene has been found to derive from carbohydrates, the

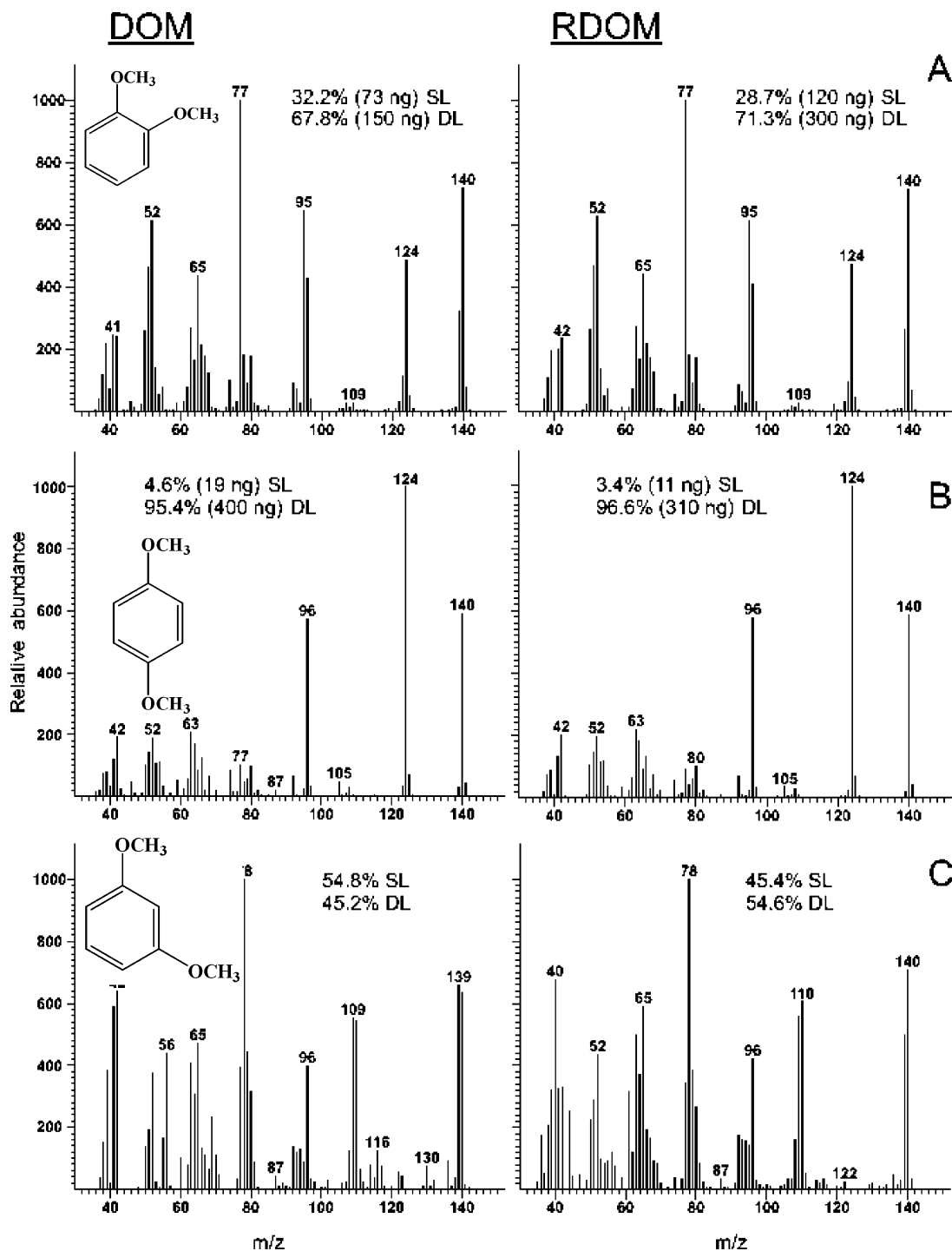


**FIGURE 6.** Mass spectra for the dimethoxy-benzene products from  $^{13}\text{C}$ -TMAH of White Clay Creek DOM. The percents are given as the amount of singly labeled (SL) and doubly labeled (DL) products, respectively, relative to the total amount of specific product. Yields are calculated as  $\text{ng L}^{-1}$ .

absence of preexisting unlabeled methoxy groups on the precursor for this compound is consistent with this source. The yield of 1,4-dimethoxy benzene decreases in the RDOM as compared to the DOM, indicating that the precursor(s) for this compound, possibly carbohydrates, are effectively degraded by passage through the bioreactors.

For the 1,3-dimethoxy benzene product, the majority derives from 3-methoxy phenol (or phenolic ether) subunits in DOM and RDOM, whereas 3-hydroxy phenol, as determined from the doubly labeled 3-methoxy phenol, accounts for less. In the RDOM, 3-hydroxy phenol (or phenolic ether) precursors account for slightly more of the product (Figure

6C). This may indicate that bacterial communities in the bioreactor can demethylate methoxy-substituted aromatic compounds. Carbohydrates do not produce detectable amounts of 1,3-dimethoxy benzene (unpublished data).

The TMAH product 1,2,3-trimethoxy benzene (peak S1) has three possible precursors: 2,5-dimethoxy phenolic ethers (presumably, from lignin), 2-hydroxy-5-methoxy phenolic ethers (presumably from degraded lignin), and 1,2,3-trihydroxy benzene, or ether analogues (phloroglucinol from degraded lignin, tannins, and carbohydrates). The dimethoxy phenolic ether precursor is apparently demethylated or degraded within the bioreactors as suggested by the decreased

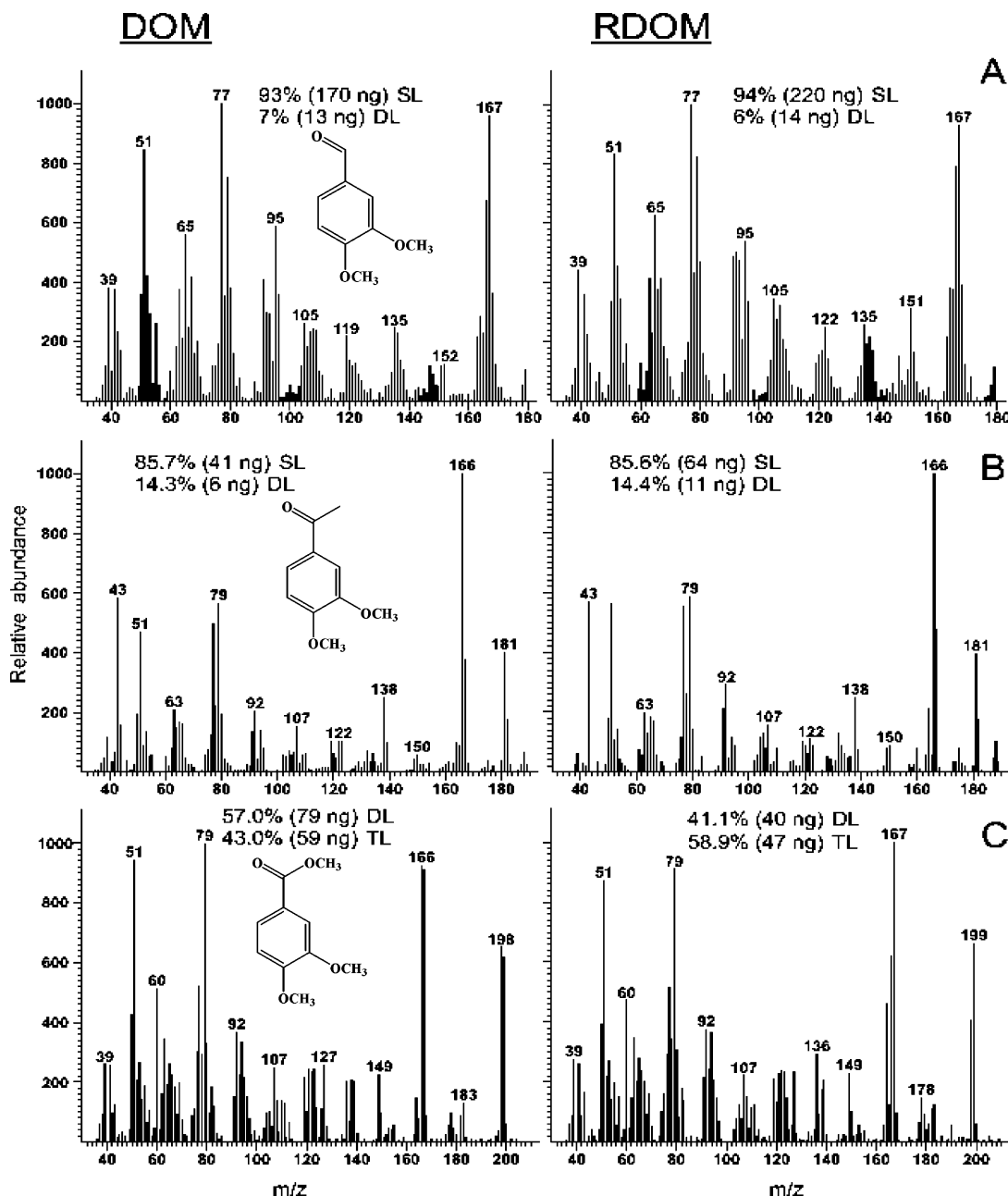


**FIGURE 7.** Mass spectra for the 3,4-dimethoxybenzaldehyde (A), 1-(3,4-dimethoxyphenyl) ethanone (B), and 3,4-dimethoxybenzoic acid, methyl ester (C) products from  $^{13}\text{C}$ -TMAH of White Clay Creek DOM. The percents are given as the amount of singly labeled (SL) and doubly labeled (DL) products, respectively, relative to the total amount of specific product. Yields are calculated as  $\text{ng L}^{-1}$ .

yield of mono-labeled trimethoxy benzene from the RDOM sample. Demethylation of the dimethoxy precursor may account for the increased concentration of the doubly labeled product with a single natural methoxy (1-hydroxy-5-methoxy phenol) group in the DOM sample. The yield from the 1,2,3-trihydroxy benzene precursor, producing the triply labeled trimethoxy benzene (not shown), also decreases substantially in the RDOM relative to the DOM, indicating carbohydrates and/or degraded lignin contribute to the BDOM.

The compound 1,3,5-trimethoxy benzene has three possible subunit precursors in DOM and RDOM, including macromolecules composed of the subunits dimethoxy phenol, hydroxy-methoxy phenol, and 3,5-dihydroxy phenol (or respective phenolic ethers). Both dimethoxy phenol and hydroxy-methoxy phenol subunits are from undetermined source macromolecules or biopolymers, and 3,5-dihydroxy phenol could be a product from carbohydrates and non-hydrolyzable tannins. There are no substantial differences

in the relative levels of label incorporation for the three precursors between DOM and RDOM. The most enriched subunit is the one deriving from 3,5-dihydroxy phenol (yielding triply labeled 1,3,5-trimethoxy benzene, not shown), which contributes about 60% of the products.

Lignin residues are best represented by  $^{13}\text{C}$ -TMAH products deriving from guaiacyl subunits (Figure 7A–C). The low signal-to-noise for the syringyl-unit-derived products precludes an acceptable level of separation from coeluting compounds, and *p*-hydroxyphenyl-derived components of lignin may not be unambiguously assigned to lignin in TMAH products. The TMAH product 3,4-dimethoxy benzaldehyde (peak G4) has two possible precursors in DOM and RDOM: 3,4-dihydroxy benzaldehyde, or its respective phenolic ether (from degraded lignin), and 3-methoxy-4-hydroxy benzaldehyde, or its respective phenolic ether (from intact lignin). It is apparent that the 3-methoxy-4-hydroxy benzaldehyde, or its respective phenolic ether, is almost exclusively the

precursor for this labeled TMAH product, contributing to 93% of the product by being doubly labeled (Figure 7A). No apparent demethylation of this precursor occurs within the bioreactors, because the degree of label incorporation does not change between DOM and RDOM. The TMAH product 1-(3,4-dimethoxyphenyl) ethanone (peak G5) also has two phenolic or phenolic ether precursors: 1-(3-methoxy-4-hydroxyphenyl) ethanone, or its respective phenolic ether (from intact lignin), and 1-(3,4-dihydroxyphenyl) ethanone, or its respective phenolic ether (from degraded lignin). Again, the product 1-(3,4-dimethoxyphenyl) ethanone is almost exclusively the singly labeled product derived from intact lignin, and only 14% of the doubly labeled product indicates that the demethylated precursor is contributing only slightly to the product (Figure 7B). There is also no change in the degree of label incorporation in this product between DOM and RDOM, indicating that demethylation of 1-(3-methoxy-4-hydroxyphenyl) ethanone does not occur during passage through the bioreactor. This indicates the lignin subunits responsible for these TMAH products are not demethylated during bioreactor degradation.

The two lignin subunit precursors that produce 3,4-dimethoxybenzoic acid methyl ester (peak G6) are 3-methoxy-4-hydroxy benzoic acid, or its respective phenolic ether (from lignin), and 3,4-dihydroxy benzoic acid, or its respective phenolic ether (from degraded lignin). In this case, methylation can occur at up to three sites, the carboxyl, which is always methylated with the labeled methyl from TMAH, and the methoxy-aromatic sites. In DOM, the doubly labeled product is dominant relative to the triply labeled product, accounting for 57% of the total product yield (Figure 7C). The RDOM, after biodegradation, contains mostly the triply labeled product as the dominant product. There is also a substantial decrease in product yield in the RDOM for both labeled products. Therefore, the lignin or degraded lignin residues responsible for these products may significantly contribute to the BDOM with bacterial demethylation of lignin occurring within the bioreactors, a phenomenon observed with model lignin compounds (43).

It is important to note that the more oxidized lignin subunits of DOM appear to be most susceptible to redistribution of labels upon bioreactor degradation. The 3,4-dimethoxybenzoic acid, methyl ester showed both a loss of concentration and a redistribution of the relative <sup>13</sup>C enrichment upon passage through the bioreactor. The other lignin markers, the 3,4-dimethoxy benzaldehyde and the 3,4-dimethoxy acetophenone, showed neither a diminution in RDOM nor a redistribution of label. Because it is known that the 3,4-dimethoxybenzoic acid, methyl ester is indicative of degraded lignin subunits, the above results suggest that such degraded units are more susceptible to demethylation reactions as are observed within the bioreactor.

## Acknowledgments

We thank Michael Gentile, Sherman Roberts, X. Cheng, Rafa Morales, Christian Collado, Charles Blount, and Chad Tricker for extensive assistance in the field and laboratory. We thank Peg Broughton for carbohydrate and tannin TMAH preparations. We thank Myrna Simpson, Yu-Ping Chin, and Samuel J. Traina for helpful comments on this manuscript. This work was funded by the NSF (DEB-9904047, DEB-0096276) and AWWARF contract #2562. Additional support at Rio Tempisquito for Gentile, Roberts, Morales, and L.A.K. was provided by the Pennswood Endowment for Environmental Research.

## Literature Cited

- (1) Findlay, S.; Likens, G. E.; Hedin, L.; Fisher, S. G.; McDowell, W. H. Organic matter dynamics in Bear Brook, Hubbard Brook Experimental Forest, New Hampshire, USA. *J. N. Am. Benthol. Soc.* **1997**, *16*, 43–46.

- (2) Hedges, J. I.; Eglinton, G.; Hatcher, P. G.; Kirchman, D. L.; Arnosti, C.; Derenne, S.; Evershed, R. P.; Kogel-Knabner, I.; de Leeuw, J. W.; Littke, R.; Michaelis, W.; Rullkotter, J. The molecularly uncharacterized component of nonliving organic matter in natural environments. *Org. Geochem.* **2000**, *31*, 945–958.
- (3) Hedges, J. I.; Keil, R. G.; Benner, R. What happens to terrestrial organic matter in the ocean? *Org. Geochem.* **1997**, *27*, 195–212.
- (4) McCarthy, M. D.; Hedges, J. I.; Benner, R. Major bacterial contribution to marine dissolved organic nitrogen. *Science* **1998**, *281*, 231–234.
- (5) Søndergaard, M.; Middleboe, M. A cross-system analysis of labile dissolved organic carbon. *Mar. Ecol.: Prog. Ser.* **1995**, *118*, 283–294.
- (6) Volk, C. J.; Volk, C. B.; Kaplan, L. A. Chemical composition of biodegradable dissolved organic matter in streamwater. *Limnol. Oceanogr.* **1997**, *42*, 39–44.
- (7) Aiken, G. *Humic Substances in Soil, Sediment, and Water; Geochemistry, Isolation, and Characterization*; John Wiley: New York, 1985.
- (8) Meyer, J. L.; Edwards, R. T.; Risley, R. Bacterial growth on dissolved organic carbon from a blackwater river. *Microb. Ecol.* **1987**, *13*, 13–29.
- (9) Moran, M. A.; Hodson, R. E. Bacterial production on humic and nonhumic components of dissolved organic carbon. *Limnol. Oceanogr.* **1990**, *35*, 1744–1756.
- (10) Moran, M. A.; Hodson, R. E. A pyrolysis-derivatization-gas chromatograph technique for the elucidation of some synthetic polymers. *Mar. Ecol.: Prog. Ser.* **1994**, *110*, 241–247.
- (11) Challinor, J. M. A pyrolysis-derivatization-gas chromatograph technique for the elucidation of some synthetic polymers. *J. Anal. Appl. Pyrolysis* **1989**, *16*, 323–333.
- (12) Challinor, J. M. Characterization of wood by pyrolysis derivatization-gas chromatography/mass spectrometry. *J. Anal. Appl. Pyrolysis* **1995**, *35*, 93–107.
- (13) del Rio, J. C.; McKinney, D. E.; Knicker, H.; Nanny, M. A.; Minard, R. D.; Hatcher, P. G. Structural characterization of bio- and geo-macromolecules by off-line thermochemolysis with tetramethylammonium hydroxide. *J. Chromatogr., A* **1998**, *823*, 433–448.
- (14) Frazier, S. W.; Nowack, K. O.; Goins, K. M.; Cannon, F. S.; Kaplan, L. A.; Hatcher, P. G. Characterization of organic matter from natural waters using tetramethylammonium hydroxide thermochemolysis GC–MS. *J. Anal. Appl. Pyrolysis* **2003**, *70*, 99–128.
- (15) Mannino, A.; Harvey, H. R. Terrestrial dissolved organic matter along an estuarine gradient and its flux to the coastal ocean. *Org. Geochem.* **2000**, *31*, 1611–1625.
- (16) van Heemst, J. D. H.; del Rio, J. C.; Hatcher, P. G.; de Leeuw, J. W. Characterization of estuarine and fluvial dissolved organic matter by thermochemolysis using tetramethylammonium hydroxide. *Acta Hydrochim. Hydrobiol.* **2000**, *28*, 69–76.
- (17) Wetzel, R. G.; Hatcher, P. G.; Bianchi, T. S. Natural photolysis by ultraviolet irradiance of recalcitrant dissolved organic matter to simple substrates for rapid bacterial metabolism. *Limnol. Oceanogr.* **1995**, *40*, 1369–1380.
- (18) Chefetz, B.; Chen, Y.; Clapp, E. D.; Hatcher, P. G. Characterization of organic matter in soils by thermochemolysis using tetramethylammonium hydroxide (TMAH). *Soil Sci. Soc. Am. J.* **2000**, *64*, 583–589.
- (19) Clifford, D. J.; Carson, D. M.; McKinney, D. E.; Bortiatynski, J. M.; Hatcher, P. G. A new rapid technique for the characterization of lignin in vascular plants: Thermochemolysis with tetramethylammonium hydroxide (TMAH). *Org. Geochem.* **1995**, *23*, 169–175.
- (20) Hatcher, P. G.; Nanny, M. A.; Minard, R. D.; Dible, S. D.; Carson, D. M. Comparison of two thermochemolytic methods for the analysis of lignin in decomposing gymnosperm wood: the CuO oxidation method and the method of thermochemolysis with tetramethylammonium hydroxide (TMAH). *Org. Geochem.* **1996**, *23*, 881–888.
- (21) Martín, F.; del Río, J. C.; González-Vila, F. J.; Verdejo, T. Thermally assisted hydrolysis and alkylation of lignins in the presence of tetra-alkylammonium hydroxides. *J. Anal. Appl. Pyrolysis* **1995**, *35*, 1–13.
- (22) Hatcher, P. G.; Clifford, D. J. Flash pyrolysis and in situ methylation of humic acids from soil. *Org. Geochem.* **1994**, *21*, 1081–1092.
- (23) McKinney, D. E.; Carson, D. M.; Clifford, D. J.; Minard, R. D.; Hatcher, P. G. Off-line thermochemolysis versus flash pyrolysis for the in situ methylation of lignin: Is pyrolysis necessary? *J. Anal. Appl. Pyrolysis* **1995**, *34*, 41–46.

- (24) Zang, X.; van Heemst, J. D. H.; Dria, K.; Hatcher, P. G. Encapsulation of protein in humic acid from a histosol as an explanation for the occurrence of organic nitrogen in soil and sediment. *Org. Geochem.* **2000**, *31*, 679–695.
- (25) Louchouart, P.; Opsahl, S.; Benner, R. Isolation and quantification of dissolved lignin from natural waters using solid-phase extraction and GC/MS. *Anal. Chem.* **2000**, *72*, 2780–2787.
- (26) Saiz-Jimenez, C. Analytical pyrolysis of humic substances: pitfalls, limitations, and possible solutions. *Environ. Sci. Technol.* **1994**, *28*, 1773–1780.
- (27) Filley, T. R.; Minard, R. D.; Hatcher, P. G. Tetramethylammonium hydroxide (TMAH) thermochemolysis: proposed mechanisms based upon the application of  $^{13}\text{C}$ -labeled TMAH to a synthetic model lignin dimer. *Org. Geochem.* **1999**, *30*, 607–621.
- (28) Kaplan, L. A.; Newbold, J. D. Measurement of streamwater biodegradable dissolved organic carbon with a plug-flow bioreactor. *Water Res.* **1995**, *29*, 2696–2706.
- (29) Newbold, J. D.; Sweeney, B. W.; Jackson, J. K.; Kaplan, L. A. Concentrations and export of solutes from 6 mountain streams in northwestern Costa-Rica. *J. N. Am. Benthol. Soc.* **1995**, *14*, 21–37.
- (30) Kaplan, L. A.; Larson, R. L.; Bott, T. L. Patterns of dissolved organic carbon in transport. *Limnol. Oceanogr.* **1980**, *25*, 1034–1043.
- (31) Cheng, X.; Kaplan, L. A. Improved analysis of dissolved carbohydrates in streamwater with HPLC–PAD. *Anal. Chem.* **2001**, *73*, 458–461.
- (32) Filley, T. R.; Hatcher, P. G.; Shortle, W. C.; Praseuth, R. T. The application of  $^{13}\text{C}$ -labeled tetramethylammonium hydroxide ( $^{13}\text{C}$ -TMAH) thermochemolysis to the study of fungal degradation of wood. *Org. Geochem.* **2000**, *31*, 181–198.
- (33) Gremm, T. J.; Kaplan, L. A. Dissolved carbohydrate concentration, composition, and bioavailability to microbial heterotrophs in streamwater. *Acta Hydrochim. Hydrobiol.* **1998**, *26*, 167–171.
- (34) Fabbri, D.; Helleur, R. Characterization of the tetramethylammonium hydroxide thermochemolysis products of carbohydrates. *J. Anal. Appl. Pyrolysis* **1999**, *49*, 277–293.
- (35) Moll, D. M.; Summers, R. S. Assessment of drinking water filter microbial communities using taxonomic and metabolic profiles. *Water Sci. Technol.* **1999**, *39*, 83–89.
- (36) Napolitano, G. E. Fatty acids as trophic and chemical markers in freshwater ecosystems. In *Lipids in freshwater ecosystems*; Arts, B. C., Wainman, M. T., Eds.; Springer-Verlag: New York, 1999.
- (37) Robson, J. N.; Rowland, S. J. Biodegradation of highly branched isoprenoid hydrocarbons – a possible explanation of sedimentary abundance. *Org. Geochem.* **1988**, *13*, 691–695.
- (38) Kawamura, K.; Ishiwatari, R.; Ogura, K. Early diagenesis of organic matter in the water column and sediments: Microbial degradation and resynthesis of lipids in Lake Haruna. *Org. Geochem.* **1987**, *11*, 251–264.
- (39) Meyers, P. A.; Leenheer, M. J.; Eadie, B. J.; Maule, S. J. Organic geochemistry of suspended and settling particulate matter in Lake Michigan. *Geochim. Cosmochim. Acta* **1984**, *48*, 443–452.
- (40) Meyers, P. A.; Ishiwatari, R. Lacustrine organic geochemistry—an overview of indicators of organic matter sources and diagenesis in lake sediments. *Org. Geochem.* **1993**, *20*, 867–900.
- (41) Ertel, J. R.; Hedges, J. I.; Perdue, E. M. Lignin signature of aquatic humic substances. *Science* **1984**, *223*, 485–487.
- (42) Ertel, J. R.; Hedges, J. I. The lignin component of humic substances: distribution among soil and sedimentary humic, fulvic, and base-insoluble fractions. *Geochim. Cosmochim. Acta* **1984**, *48*, 2065–2074.
- (43) Dagley, S. Catabolism of aromatic compounds by microorganisms. *Adv. Microb. Physiol.* **1971**, *6*, 1–46.
- (44) Kawakami, H. Degradation of lignin-related aromatics and lignins by several pseudomonads. *Proc. Int. Sem. Lignin Biodegrad.: Microbiol., Chem., Pot. Appl.* **1980**, *2*, 103–125.

Received for review April 2, 2004. Revised manuscript received September 21, 2004. Accepted December 10, 2004.

ES0494959